



Thermally annealed biochar assisted nanofluid as quenchant on the mechanical and microstructure properties of AISI-1020 heat-treated steel—a cleaner production approach

R. Arularasan¹ · K. Babu¹

Received: 26 May 2021 / Revised: 24 June 2021 / Accepted: 3 July 2021 / Published online: 11 July 2021
© The Author(s), under exclusive licence to Springer-Verlag GmbH Germany, part of Springer Nature 2021

Abstract

To improve the mechanical and microstructure properties of low carbon steel (AISI 1020), a thermally annealed biochar (TAB)-aided quenchant was used in this study. The primary goal of this research was to see how effective it was to use a low-cost, thermally conductive (10^3S/m) annealed biochar to improve the mechanical and microstructure of a quench hardened steel workpiece as a quenchant. The quenching procedure was carried out in this analysis with pure distilled water and 0.25, 0.5wt% annealed biochar dispersed distilled water nanofluids. The quenched sample with 0.25wt% biochar nanofluid had a faster cooling rate, lower surface roughness, and a higher hardness value from the center to the edges, according to the findings. Similarly, the specific wear rate and coefficient of friction (COF) of 0.25wt% biochar-aided quenchant are $0.0058\text{mm}^3/\text{Nm}$ and 0.44, respectively. Furthermore, the martensite microstructures in the 0.25wt% biochar nanofluid quenched workpiece are more refined than the distorted martensite in the 0.5wt% biochar nanofluid quenched workpiece. These low-cost, high-performance, and environmental friendly nanofluids made with annealed biochar may be a cheaper alternative to nanofluids made with other high-cost carbon allotropes like carbon nanotubes (CNTs), graphene, and fullerene.

Keywords Biochar · Nanofluid · Quenching · Microstructure · Mechanical properties

1 Introduction

Biochar has sparked the scientific community's curiosity in recent decades, not just for soil and fuel applications, but also as a carbonaceous source for high-value-added applications [1, 2]. Biochar is a good contender to become the carbon base for a new age in materials science because of its low-cost and low environmental footprint [3]. The use of biochar in polypropylene-based composites was investigated by Noori et al. [4]. They demonstrated that biochar is an excellent option for toughening a variety of thermoset and thermoplastic polymeric matrixes. Similarly, Giorcelli et al. [5] demonstrated that biochar can be used as a substitute for high-performance carbon fillers such as CNTs, resulting in improved mechanical properties. However, owing to the limited scale and low consistency of the graphitic domains,

biochar's electrical and thermal properties lag well behind those of graphene and carbon nanotubes (carbon allotropes) [6]. By pyrolyzing biochar at temperatures above $800\text{ }^\circ\text{C}$ or postproduction thermal annealing at temperatures similar to or above $900\text{ }^\circ\text{C}$, the thermal conductivity of biochar could be improved up to 1.33 W/mK [7, 8]. Owing to the minimal production of volatile organic matter during the early stages of pyrolysis, this efficient method is simpler to handle. Furthermore, owing to the likelihood of using sintering ovens instead of pyrolytic devices, higher temperatures could be achieved using the postproduction annealing technique. The configuration and reorganization of graphitic domains by turbostratic rearrangement occurs at temperatures up to $1000\text{ }^\circ\text{C}$, resulting in a drastic rise in electrical conductivity [9, 10].

Quenching is one of the most important heat treatment methods for hardening steels. Quenching is a fast cooling mechanism in which the rate of heat transfer and cooling are important parameters. It determines the steel components' mechanical and metallurgical properties. While quenching, three distinct cooling mechanisms (film boiling, nucleate boiling, and convective boiling) are generated. Immersion

✉ R. Arularasan
rarulphd@rediffmail.com

¹ Department of Mechanical Engineering, SSN College of Engineering, Chennai 603110, India

quenching is a form of quenching in which steel components are heated to an austenitizing temperature and then cooled quickly by immersing them in quenchants. Since the carbon content defines the steel's hardness, carbon steels are commonly subjected to quenching. Carbon steels are divided into three categories based on their carbon content: low, medium, and high. The importance of using low carbon steels (0.04wt% to 0.30wt%) is that they have sufficient strength for constructing steel frames on construction sites, are inexpensive, and can be used for machinery components. The heat transfer rate by quenching is precisely determined by surface temperature, thermo-physical properties of the saturated liquid, size and form of the substance, and roughness of the heating surface with carbon steels. Several previous studies examined the microstructure and mechanical properties of carbon steels quenched in various quenching media, as well as the heat transfer rate of various quenching media. The industrial steel quenched with bio quenchants was studied by Fernandes et al. [11]. The author discovered that sunflower oil has the highest heat transfer coefficients compared to Castrol oil, which has the lowest heat transfer coefficient. From highest to lowest order, the heat transfer coefficient is as follows: mineral oil > groundnut oil > castor oil > sunflower oil > coconut oil > palm oil > mineral oil > groundnut oil > castor oil. Prasanna et al. [12] used CNT nanofluids to conduct quenching tests on stainless steel to assess the effect of surface heat flux and the optimal CNT concentration. They found that when quenching in CNT nanofluids, the heat transfer rate was high before the CNT concentration reached 0.5wt%, then it decreased as the CNT concentration increased. The researchers have discovered that the heat transfer rate of the nanofluid generated without surfactant is higher than that of the nanofluid produced with surfactant. Similarly, Giordani et al. [13] investigated the microstructure and metallurgical behavior of two separate steel plates quenched conventionally and intensively, with and without carburized surfaces (AISI 1020 and AISI 8620). Researchers discovered that rapid quenching of carburized AISI 1020 steel outperformed traditional quenching in any way. Plain carbon steels are usually devoid of Al and Ti elemental additions, but a grain size of at least 6–8 is needed for a better performance. Sayed et al. [14] conducted an experimental analysis on AISI 1020 steel using a heat treatment method that included annealing, hardening, and normalizing at 850 °C, and found that the differences in microstructures are caused by substantial differences in the effect of cooling rate and carbon content. Babu et al. used CNT nanofluid with and without surfactant as a quenchant in a quenching experiment on low carbon steel AISI 1010. The researcher discovered that the probe quenched without surfactant has a high hardness. The obtained microstructure corresponds to mechanical properties [15]. The effect of TiO₂ nanoparticles in distilled water was examined by Prayogo et al. [16].

The cooling characteristics of ball-milled micro-sized TiO₂ powder and nano-sized TiO₂ particles were contrasted in a micro/nanofluid in this study. The micro/nanofluids were made by combining 0.1%, 0.3%, and 0.5% of both micro- and nano-sized particles in 100 ml of distilled water. The sample quenched with 0.5% inclusion of nano-sized particle in nanofluid had the largest amount, up to 691 HV, nearly 100 HV higher than a water-quenched sample with a hardness of 598 HV, indicating that the cooling rate in the nanofluid was much higher. As a result, heat treatment will alter the microstructure and mechanical properties of any ferrous material with adequate carbon content. The quenching medium, on the other hand, will determine the microstructure of hardened steel.

According to the previous literature, the cooling effect of the quenching medium plays an important role in efficient heat control during the heat rejection step in the hardening of ferrous alloys. There has been a great number of study into the use of CNT and graphene as functional cooling materials for efficient quenching. However, as previously mentioned, these carbon allotropes are extremely expensive. In addition, the availability is not as good as the biochar material. According to research, graphitized biochar particles have strong electrical and thermal properties, allowing them to replace high-cost fillers like CNTs and graphene in cooling applications. It should be remembered that no research has been done on the efficacy of biochar aided quenchants and their use in the heat treatment process. This study aims to investigate the efficiency of biochar addition as a functional cooling agent for the quenchants in the heat treatment process, based on a possible research gap. In this analysis, related outcomes such as surface roughness, hardness, and microstructural changes were also investigated. These low-cost bioroute-derived abundant cooling materials (biochar) may be a new realm of several new research scopes with high economic indexes and woos environmentally sustainable cleaner production systems.

2 Experimental procedure

2.1 Design of workpiece

A special probe type workpiece pattern is used to study the quenching effects on the workpiece. The workpiece is machined to a diameter of 20 mm and a length of 50 mm from carbon steels of grade AISI 1020, and a thread of 4 mm depth is drilled into the middle of the quench workpiece probes using an M6 drill bit, as well as a stem of 10 mm stainless steel that is welded by M6 bolt at one end to hold the quench workpiece probe. For temperature calculation during quenching, two insulated K-type thermocouples (TC₁ and TC₂) with a diameter of 1 mm were held

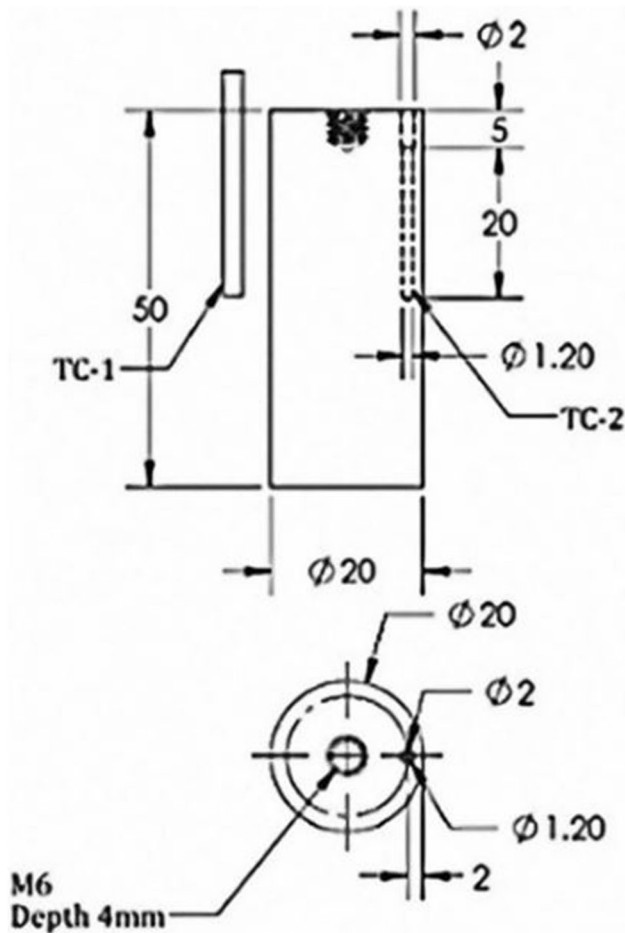


Fig. 1 Quench workpiece probe design

Table 1 Chemical composition of AISI 1020

Element	C	P	S	Mn
Weight%	0.20	0.024	0.012	0.648

inside the workpiece. From 2 mm away from the edge, a 2-mm drill bit was used to make a depth of 5 mm, and a 1.2-mm drill bit was used to make a depth of 20 mm for positioning TC₂. To avoid temperature errors during heating in a furnace, COREFIX, a commercial adhesive paste, was used to insert the TC₂ in the workpiece, and it was then allowed to cure at room temperature for 24 h. TC₁ is positioned diametrically opposite TC₂ on the workpiece board. Figure 1 depicts the AISI 1020 quench workpiece structure. Table 1 shows the chemical composition of carbon steels of grade AISI 1020 as determined by optical emission spectroscopy (OES) at Micro, Small & Medium Enterprises (MSME) in Chennai, India. Wavelength range of 200–1100 nm, resolution of 0.6–0.7 nm, grating (lines/mm) of 300 lines/mm, and sensitivity of $> 1 \times 10^5$

counts/ μ W per ms integration time were used as process parameters.

2.2 Materials

2.2.1 Preparation of annealed biochar

There are two phases in the annealed biochar preparation procedure. The separated rice husk from the paddy was first put through a low temperature pyrolysis operation. In this process, the rice husk is fully burned at 400 °C in a controlled environment. The burnt rice husk is then taken to room temperature and powdered for about 30 min in a low-energy ball mill. Second, the fine-powdered rice husk was annealed in order to increase the number of graphitic domains and thus improve thermal conductivity. The pulverized fine biochar powder was annealed in a vacuum electric furnace under nitrogen atmosphere, with a heating rate of 100 °C/h, a dwell time of 60 min at a maximum temperature of 1000 °C, and cooling to room temperature inside the furnace itself. A low-energy ball mill was used to pulverize the room temperature-cooled annealed biochar particles for around 30 min. Pyrolysis and annealing is used to create fine-sized biochar particles of around 800 nm [17, 18]. Figure 2 depicts the decomposition of biochar particle formation in stages.

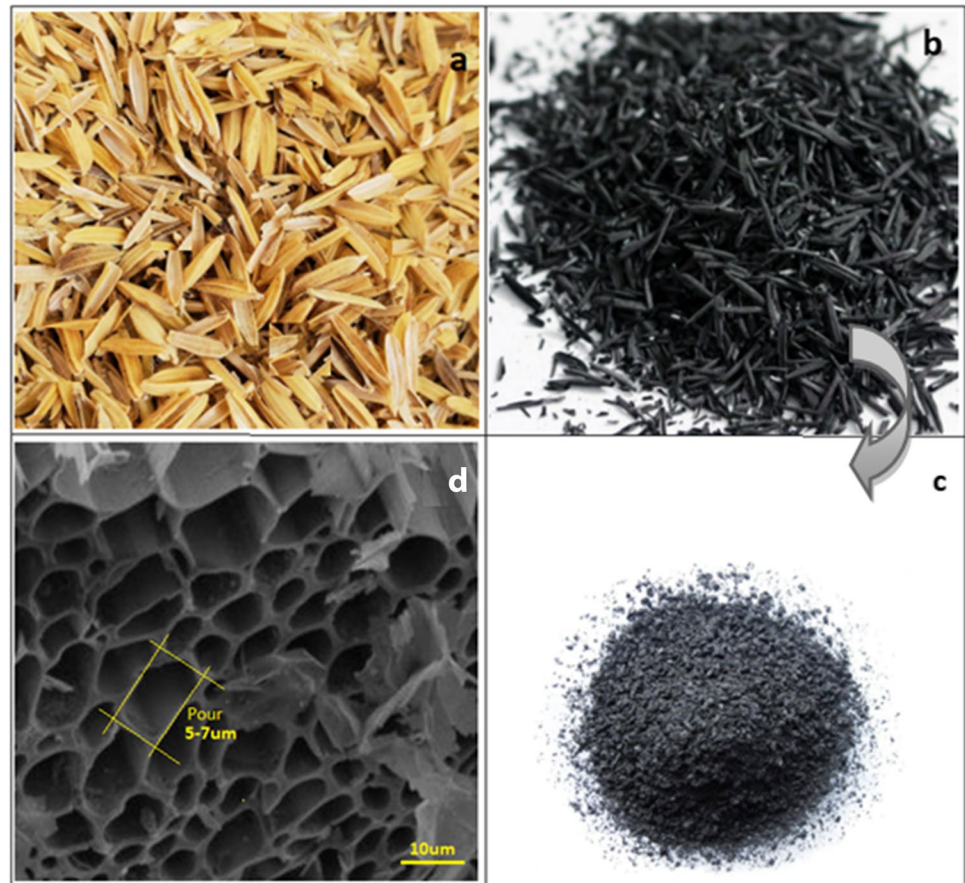
2.2.2 Biochar-activated nanofluid

To make nanofluids, the furnace annealed graphitized turbostratic rearranged biochar was directly dispersed in distilled water. The sonication mechanism is used to scatter the particles in distilled water. In this experiment, the sonicator was a probe style sonicator (Roopetsonic Ultrasonic Ltd, Model USG-1000). Biochar nanofluids are formulated in two concentrations: 0.25 wt% biochar nanofluid and 0.5 wt% biochar nanofluid. To get even dispersion of biochar particles, the 5gm and 10gm biochar particles were weighted and then dispersed in 2L of distilled water using the sonication procedure for 30 min at 20 kHz [19].

2.3 Quenching process

For each trial, a new AISI-1020 workpiece probe was used to assess the efficacy of the quenching operation. Workpiece probes were heated to 850 °C in a vertical tubular furnace with a burette stand (Hitech Ceramics, Chennai, India). The quench workpiece probe is adjusted to hang in the furnace heating zone using a clamp and a burette stand. Glass wool is mounted at the top of the furnace to avoid heat loss during the heating process. The quench workpiece probe was soaked for 15 min before being removed from the burette stand and immediately submerged in a beaker containing 2 l

Fig. 2 Images of **a** rice husk, **b** pyrolysis rice husk, **c** pulverized rice husk and **d** SEM image of rice husk fine powder



of distilled water held at room temperature with the workpiece axis vertical. The same experiment was carried out for two separate biochar nanofluid concentrations (0.25wt% and 0.5wt%). The data acquisition system (Agilent–Model No.34972A) was used to capture time–temperature data every 0.1 s before the workpiece probe temperature reached 300 °C [20].

3 Characterization

The quenched hardened workpiece probes were subjected to further characterization. The quenched workpiece probes were tested by a surface roughness tester (Surftest SJ-210-Series 178-Portable) at five separate passes to determine the average Ra values. Similarly, Vickers hardness measuring system (Wilson Wolpert MVD 410) was used to calculate the hardness value from core to edge gap in mm (0, 2, 4, 6, 8, 9, 9.5, and 10) at 0.5 kgf load. Four measurements were taken in each interval, and the average value was determined. A pin-on-disc setup also reveals the wear activity of the quenched steel workpiece probe (Magnum Engineers India Pvt. Ltd). The pin-on-disc has a 165-mm wear disc, a 100–2000 rpm disc speed, and a standard load

of 5–200 N. As method parameters, a load of 10 N, a sliding speed of 800 rpm, and a sliding distance of 400 m were maintained. The wear resistance of quenched specimens was tested using circular specimens with a 8-mm diameter and a 3-mm length. An optical microscope was used to examine the microstructure of the quenched workpiece in three distinct mediums (Dewinter victory inverted model IM364). The microstructure of the quenched workpiece was recorded in three separate locations. The quenched workpieces were sectioned precisely at the middle of their axis using a band saw with spray coolant, and it was hot mounted to handle. The specimens were then grained using abrasive sheet SiC (Silicon Carbide) grit scale of 80, 120, 240, 320, 600, 800, and 1200 using a motorized disc spinning grinding wheel. After finely grinding the specimen, it was polished on velvet cloth with enough aluminum oxide slurry poured through a spinning disc to remove the scratch and achieve a mirror-like finish. The chemical etching was done manually by immersing the specimen in a 2wt% nital (nitric acid and alcohol) solution, then removing it and leaving it to dry for 5–10 s. Following that, the sample was scanned. A scanning electron microscope, HITACHI, S1500, JAPAN, was used to scan the high resolution micrography images of the quenched workpiece.

4 Result and discussion

4.1 Cooling curve and cooling rate

Figure 3 shows the cooling curve of the quenched AISI 1020 steel workpiece probe derived from time–temperature data for TC₁ and TC₂. When the workpiece probe is completely submerged directly after extracting it from the furnace until the temperature decreases to room temperature, the readings in TC₁ and TC₂ indicate the difference in readings. The three phases of immersion quenching were: vapor or film boiling, transition boiling, and nucleate boiling. The TC₁ curve depicts the temperature drop from surface to core at 2 mm below the workpiece probe’s surface, while the TC₂ curve depicts the temperature drop from surface to core at 2 mm below the workpiece probe’s surface. The temperature reported at TC₁ has a more random decrease from vapor boiling to nucleate boiling stage than the temperature recorded at TC₂, so the recorded TC₁ and TC₂ temperature data is linked to its cooling rate, which is plotted in Fig. 4. According to the line table, a 0.25wt% biochar nanofluid has a faster cooling rate than other quenching media.

4.2 Surface roughness

The biochar nanoparticles adhere to the heated surface after being quenched in nanofluid. Figure 5 shows that, of the various quenching mediums, the workpiece probe quenched in water has the highest surface roughness value. This higher value is attributed to a rapid heat rejection from the surface, which results in atom eviction due to very high temperatures. Furthermore, since the water was unable to sustain a vapor blanket for an extended period of time, unequal heat rejection happened on the atmosphere, resulting in an uneven surface [21]. Moreover, the rapid cooling induced micro hair line cracks on the surface and resulted poor surface

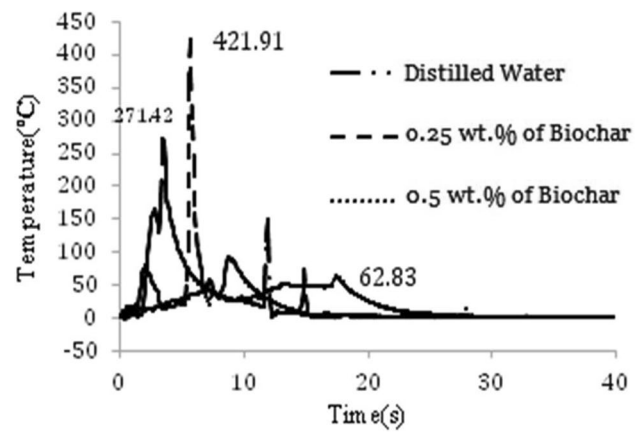


Fig. 4 Cooling Rate for TC2

finish. Moreover, the hair line cracks some time probably grown up and the material is fled off from the workpiece. The workpiece probe quenched in biochar nanofluid containing 0.25wt% annealed biochar, on the other hand, has less surface roughness than the distilled water quenchant. A 0.5wt% annealed biochar-activated distilled water nanofluid showed similar changes. Both the designations of quenchant rendered of 0.25 and 0.5wt% of annealed biochar showed a decrease in surface roughness of 40% and 32%, respectively. Because of the extended vapor blanket period, the workpiece probe quenched in biochar nanofluid has a lower surface roughness and damage. More biocarbon penetration from the fluid onto the surface may have been avoided by the extended vapor blanket. The array of shell-like structure on the biochar contains air, which has poor thermal conducting and store lot of heat energy. Thus, the vapor blanket stage is lasting for long time and eventually improved the cooling effect. Moreover, the evaporation temperature of biochar is also very high, thus it can be withstand for

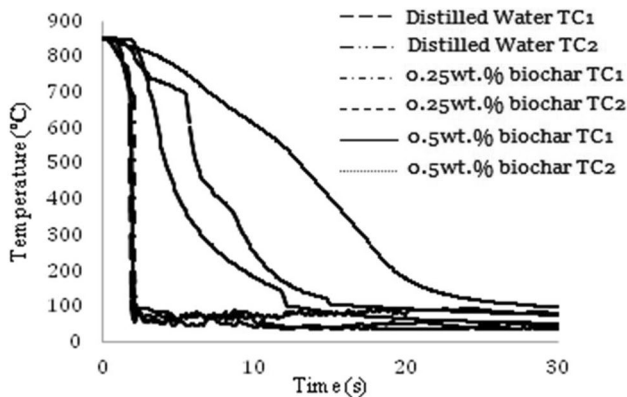


Fig. 3 The cooling curve for TC1 and TC2

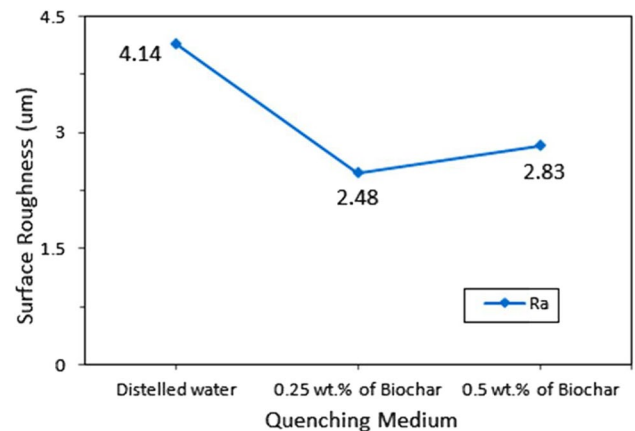


Fig. 5 Surface roughness (R_a) measurement values

larger temperature and maintains the same state for a long period. Furthermore, the extended vapor blanket decreased heat loss from the atmosphere, lowering surface energy and preventing foreign particles from penetrating. Thus, the surface roughness was greatly decreased as a result of this phenomenon [22].

4.3 Hardness survey

The hardness line chart values of liquid water, 0.25wt% annealed biochar, and 0.5wt% annealed biochar quenched workpiece probe are seen in Fig. 6. The hardness of distilled water is higher near the edge and lowers near the center, according to the line chart, and then rises near the edge. This is because of rapid cooling and sudden boiling of distilled water. Since the distilled water is not equipped with cooling medium, it gets evaporated above 100 °C. Thus, the hardness on the workpiece probe is significantly higher from the tip to the core. However, in 0.25wt% biochar nanofluid, which is similar to distilled water, the hardness value is elevated at the core but drops abruptly at the end. This is because of long lasting vapor blanket around the workpiece. Thus, the grain refinement is very fine and offered lesser hardness. While in 0.5wt% biochar nanofluid, the hardness

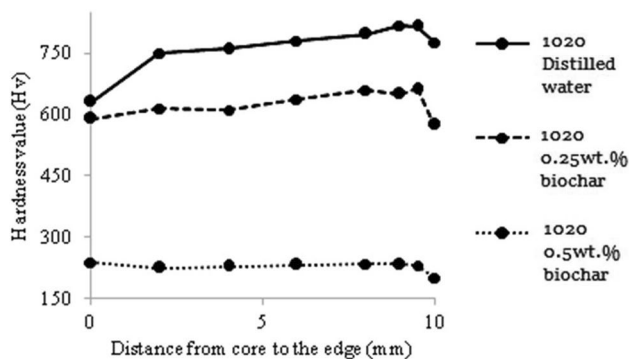


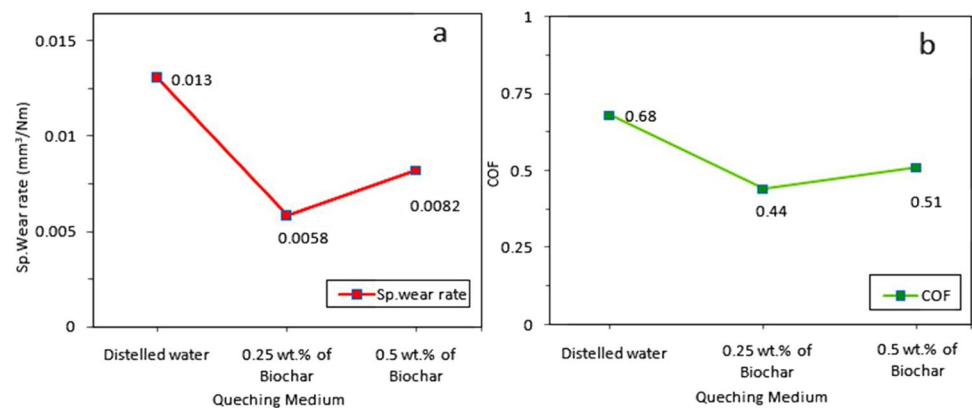
Fig. 6 Hardness survey (Hv) measured value

value is very low from the core to the edge. Because of the even deposition of biocarbon on the porous surface, the hardness value of the 0.25wt% biochar-assisted nanofluid is high at 0.5 mm from the tip, whereas the quenching and cooling rate is high for 0.25wt% annealed biochar assisted nanofluid. The cooling rate and hardness value of 0.5wt% annealed biochar nanofluid both are low. This is due to the gradual cooling of the film before it reaches the end of the boiling process. The long lasting of vapor film maintains the heat rejection on the workpiece material and allows the grains to grow further. Large grains are directly proportional to hardness and grain refinement. Thus, lower hardness is experienced. Since the grain refinement is directly impacting with the microstructures, the changes in the cooling rate and cooling medium had an effect on the surface hardness and core hardness values [23].

4.4 Wear behavior

Figure 7 depicts the wear rate and coefficient of friction values of heat-treated AISI steel when quenched in various media. The specific wear rate of the distilled water-quenched workpiece probe is 0.013mm³/Nm, with a COF of 0.68. The highly distorted grains on the quenched surfaces of the workpiece are due to this relatively greater wear volume. The hardness and extremely distorted martensite are retained on the high brittle gained quenched surface. As a result, when the surface of the workpiece is exposed to the abrasion disc, extremely brittle particles from the workpiece are ejected and trapped between the abrasion disc and the workpiece material, facilitating three and two body abrasion wear mechanisms and resulting in increased abrasion loss [24]. However, the 0.25wt% biochar-activated distilled water nanofluid, on the other hand, had a high persistent wear resistance. The sp.wear rate was 0.005mm³/Nm, and the COF was 0.44. Also after the rubbing action, the refined martensite in the quenched surface retains uniform wear resistance. This improvement is attributed to the uniform quenching caused by the lasted vapor blanket across

Fig. 7 Wear behaviour of quenched workpiece probe **a** sp.wear rate and **b** COF



the surface created by the biochar. The stress-free (refined martensite) grains in the workpiece maintain surface integrity by absorbing large vibrations and thrust forces. Thus, uniform and lower wear resistance is observed. A similar change was seen in the 0.5wt% biochar-distributed nanofluid as well. However, the wear loss and COF have shifted somewhat. The measured sp.wear rate was $0.0082\text{mm}^3/\text{Nm}$, with a COF of 0.51. This marginal increment is the cause for sustained cooling, which may facilitate large grains and higher carbon particle penetration, which may be evicted as abrasion begins. In addition, the evicted carbon particle stuck between the abrasion disc and possibly formed as a flake-like structure. These flakes further improve the wear loss during the abrasion process. Overall, the biochar-activated distilled water-based nanofluid outperformed the as-received distilled waste quenching method in terms of wear resistance [25].

4.5 Microstructures

The optical microscopic images of distilled water, 0.25 and 0.5wt% biochar-activated nanofluid quenched workpiece probe are seen in Fig. 8. The phases of ferrite, coarse and fine pearlite, retained austenite, and bainite/martensite were found in the three quenchants. Fine pearlite is formed when biochar nanofluid is quenched, while coarse pearlite is formed when distilled water is used. Retained austenite is caused by diffusion-less carbon, which prevents austenite from transforming into martensite. The observed martensite phase of 0.5wt% carbon steel was compared to that of

0.3wt% carbon steel in terms of cooling rate and prior austenite grain size; the higher dislocation density obtained for 0.5wt% carbon was due to the addition of biocarbon content from biochar, which increased the retained austenite volume and strengthened the steel; decohesion often occurred [26, 27].

QUANTIMENT, image analysis software, was used to quantify the stages. The edges of the three separate quenchants were analyzed, and the percentage of phases determined, as seen in Fig. 9’s column table. Since the volume of pearlite is maximum when quenched in distilled water and the volume of ferrite is lowest, there is a risk of surface fracturing and cracks [28]. Compared with both 0.25wt% and 0.5wt% biochar nanofluid quenched workpiece probes, the

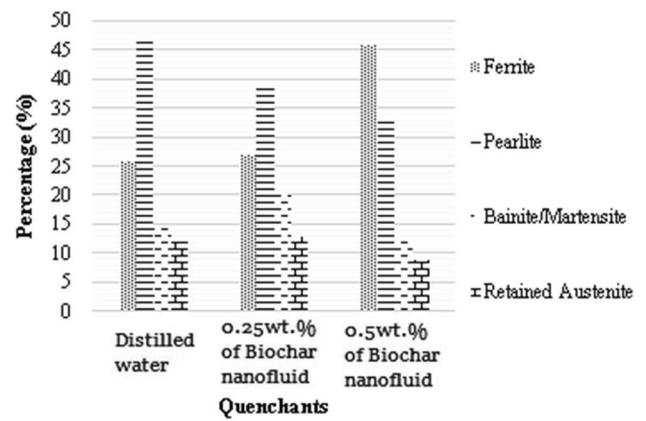
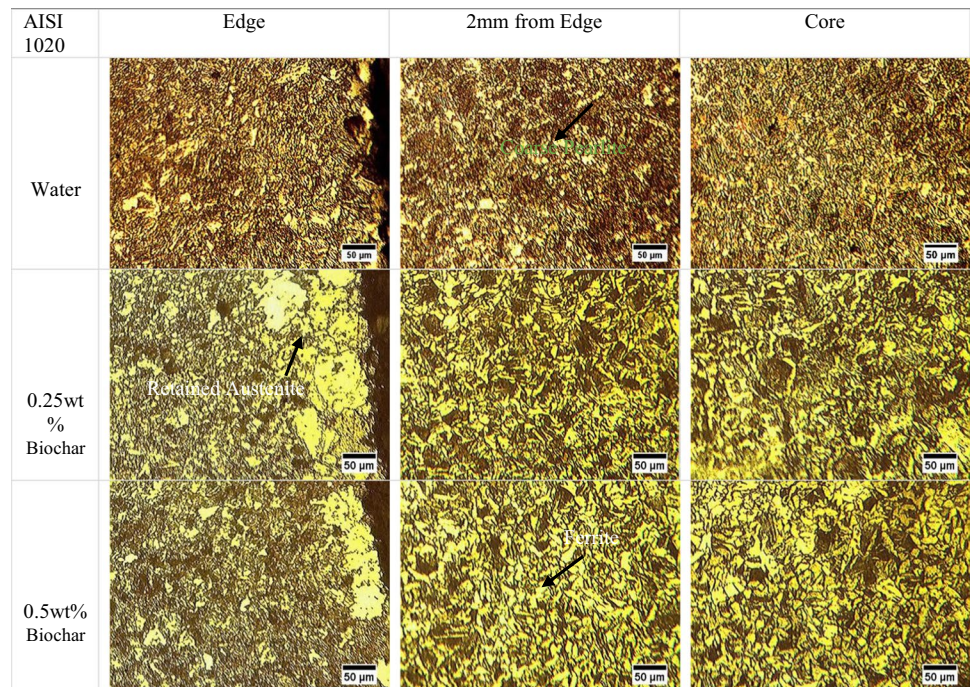


Fig. 9 Phase percentage of the quenchants

Fig. 8 The optical microstructure of the different quenched medium



0.25wt% biochar-assisted fluid has a better volume of ferrite, pearlite, and bainite/martensite. The 0.5wt% biochar-aided quenchant, on the other hand, has a higher amount of ferrite due to the slower cooling rate. The 0.25wt% biochar-assisted quenchant, on the other hand, has greater microstructures than the 0.5wt% biochar-assisted nanofluid.

Figure 10 displays images of quenched specimens taken using a scanning electron microscope (workpiece probe). More bainite and martensite phases are visible in the microstructure, with a small volume of carbide particle precipitating. The carbide particle formed during the decomposition of martensite and was replaced by ferrite grains where the carbide particle formed before transitioning to the lath martensite. Due to an incorrect carbon diffusion gap, there was a retained austenite phase at the edge, where the austenite did not turn into a full martensite phase [29, 30]. The different quenchants change the volume of the phases, as can be seen in the figure. The series distilled water > 0.25wt% biochar nanofluid > 0.5wt% biochar nanofluid were found to be a better one at the edge, core, and 2 mm from the edge, where the bainite/martensite and retained austenite phases were found.

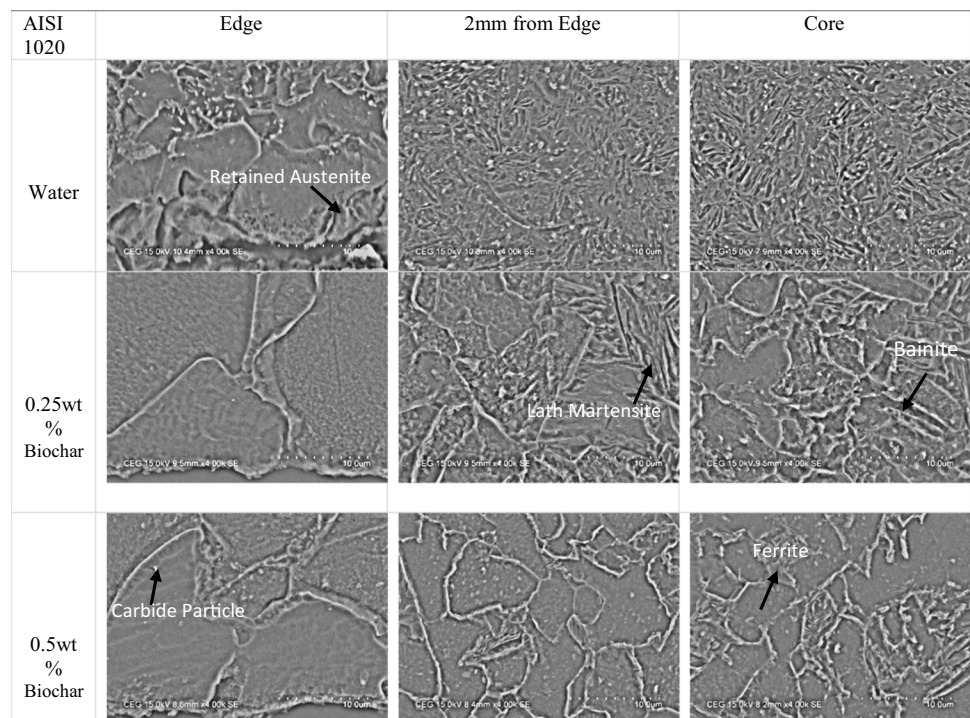
5 Conclusions

The quenching in distilled water and annealed biochar aided nanofluids on AISI 1020 steel were tested in this study. The mechanical and microstructure properties of

distilled water, 0.25wt% biochar nanofluid, and 0.5wt% biochar nanofluid quenchants were reported. The following are the most important findings of this research:

- The cooling curve and cooling rate probes of the quenched workpiece were studied, and a fast and uniform cooling curve was obtained for 0.25wt% biochar-assisted distilled water nanofluid.
- The end of the film boiling and nucleate boiling stages determined whether the cooling should be quicker or slower. The cooling rate for 0.25wt% biochar nanofluid, which was chosen between film and nucleate boiling, is higher.
- The surface roughness value for 0.25wt% biochar-aided nanofluid is smaller at 2.48 μm , while distilled water has a higher surface roughness of 4.14 μm .
- The hardness survey findings of distilled water-quenched workpiece probes had the lowest hardness value at the core (632) HV, eventually rose from the core, and peaked at 9.5 mm (816) HV. As compared to 0.25wt% and 0.5wt% annealed biochar nanofluid quenched workpiece probes, 0.5wt% annealed biochar nanofluid quenched workpiece probes had the lowest hardness value at the center (240) HV and 0.25wt% biochar nanofluid quenched probes workpiece had the highest hardness value at 0.5 mm (663) HV from the tip. As a result, 0.25wt% biochar nanofluid was found to be effective in terms of hardness.

Fig. 10 SEM analysis of the different quenched medium



- Quenched specimens have ferrite, coarse pearlite, coarse pearlite, bainite, martensite, and retained austenite, according to optical and SEM microstructure. There is a lot of pearlite, a little retained austenite, and bainite/martensite in the workpiece probes quenched in distilled water. The probe quenched with biochar nanofluid (0.25wt%) has a microstructure that is superior to distilled water, with lath type martensite, bainite, little retained austenite, and more carbide crystals.
- Finally, 0.25wt% annealed biochar nanofluid effectively achieved the higher cooling rate, least surface roughness, greater hardness content, and refined grains in the microstructures.
- Thus, the addition of biochar into the distilled water could be the noteworthy process in order to produce high-performance functional hardened steels with desirable mechanical and microstructure properties. Moreover, this method of utilizing the bio-derived substances as an engineering material could improve the process and cost efficiency and lead to a cleaner way for production.

References

- Giorcelli M, Bartoli M, Sanginario A, Padovano E, Rosso C, Rovere M, Tagliaferro A (2021) High-temperature annealed biochar as a conductive filler for the production of piezoresistive materials for energy conversion application. *ACS Appl Electron Mater* 3(2):838–844
- Cha JS, Park SH, Jung SC, Ryu C, Jeon JK, Shin MC, Park YK (2016) Production and utilization of biochar: a review. *J Ind Eng Chem* 40:1–15
- Bartoli M, Giorcelli M, Jagdale P, Rovere M, Tagliaferro A (2020) A review of non-soil biochar applications. *Materials* 13(2):261
- Noori A, Bartoli M, Frache A, Piatti E, Giorcelli M, Tagliaferro A (2020) Development of pressure-responsive polypropylene and biochar-based materials. *Micromachines* 11(4):339
- Giorcelli M, Savi P, Khan A, Tagliaferro A (2019) Analysis of biochar with different pyrolysis temperatures used as filler in epoxy resin composites. *Biomass Bioenerg* 122:466–471
- Savi P, Yasir M, Bartoli M, Giorcelli M, Longo M (2020) Electrical and microwave characterization of thermal annealed sewage sludge derived biochar composites. *Appl Sci* 10(4):1334
- Usowicz B, Lipiec J, Łukowski M, Marczewski W, Usowicz J (2016) The effect of biochar application on thermal properties and albedo of loess soil under grassland and fallow. *Soil Tillage Res* 164:45–51
- Bartoli M, Nasir MA, Jagdale P, Passaglia E, Spiniello R, Rosso C, Giorcelli M, Rovere M, Tagliaferro A (2020) Influence of pyrolytic thermal history on olive pruning biochar and related epoxy composites mechanical properties. *J Compos Mater* 54(14):1863–1873
- Eom Y, Son SM, Kim YE, Lee JE, Hwang SH, Chae HG (2019) Structure evolution mechanism of highly ordered graphite during carbonization of cellulose nanocrystals. *Carbon* 150:142–152
- Downie A, Crosky A, Munroe P (2009) Physical properties of biochar, biochar for environmental management: science and technology. Lehmann J, Joseph S (eds), Earthscan Ltd., London
- Fernandes P, Narayan Prabhu K (2008) Comparative study of heat transfer and wetting behaviour of conventional and bio-enchants for industrial heat treatment. *Int J Heat Mass Transf* 51(3–4):526–538
- Babu K, Prasanna Kumar TS (2011) Effect of CNT concentration and agitation on surface heat flux during quenching in CNT nanofluids. *Int J Heat Mass Transf* 54(1–3):106–117
- Giordani T, Clarke TR, Kwietniewski CEF, Aronov MA, Kobasko NI, Totten GE (2013) Mechanical and metallurgical evaluation of carburized, conventionally and intensively quenched steels. *J Mater Eng Perform* 22(8):2304–2313
- Hossain SS, MaksudulIslam Md, SajibulAlamBhuyan Md (2014) *Global J Res Eng A Mech Mechs Eng* 14:35–39
- Babu K, Arularasan R, SrinathRamkumar S (2017) *Mater Today Proc* 4:11044–11049
- Prayogo IF, Muhammad F, Rakhman D, Putra WN, Harjanto S (2019) Effect of titanium dioxide particle size in water-based micro/nanofluid as quench medium in heat treatment process. In *IOP Conference Series: Materials Science and Engineering* 547(1) p 012064. IOP Publishing
- Ferreira GF, Pierozzi M, Fingolo AC, da Silva WP, Strauss M (2019) Tuning sugarcane bagasse biochar into a potential carbon black substitute for polyethylene composites. *J Polym Environ* 27(8):1735–1745
- Matta S, Bartoli M, Frache A, Malucelli G (2021) Investigation of different types of biochar on the thermal stability and fire retardance of ethylene-vinyl acetate copolymers. *Polymers* 13(8):1256
- Jagatheesan K, Babu K (2020) Taguchi optimization of minimum quantity lubrication turning of AISI-4320 steel using biochar nanofluid. *Biomass Convers Biorefinery* 1–8
- Baday Ş, Başak H, Sönmez F (2020) Investigation and optimization of surface roughness with experimental design methods by turning of AISI-1050 after spheroidization heat treatment. *SN Applied Sciences* 2(12):1–13
- Li J-Q, Mou L-W, Zhang J-Y, Zhang Y-H, Fan L-W (2018) Enhanced pool boiling heat transfer during quenching of water on superhydrophilic porous surfaces: effects of the surface wickability. *Int J Heat Mass Transf* 125:494–505
- Alfatlawi SHA (2018) Influence the quenching and tempering on the microstructure, mechanical properties and surface roughness, of medium carbon steel. *Iraq J Mech Mater Eng* 18(1):125–135
- Yahya SS, Harjanto S, Putra WN, Ramahdita G, Kresnodrianto, Mahiswara EP (2018) Characterization and observation of water-based nanofluids quench medium with carbon particle content variation. In *AIP Conference Proceedings* 1964(1) 020006. AIP Publishing LLC
- Chintha AR (2019) Metallurgical aspects of steels designed to resist abrasion, and impact-abrasion wear. *Mater Sci Technol* 35(10):1133–1148
- Radhiyah AA, Nurziela K (2020) Effect of TiO₂ nanofluid and hybrid TiO₂ nanofluid on mechanical properties of steels for automotive applications. *J Phys Conf Ser* 1529(5) 052036. IOP Publishing
- Dey D, Sahu DS (2021) A review on the application of the nanofluids. *Heat Transfer* 50(2):1113–1155
- Nayak UV, Prabhu KN (2019) Quench Cooling performance-hardness correlation for AISI 1045 and 1090 steels. *Mater Perform Charact* 8(1):135–150
- Ramesh G, Narayan Prabhu K (2014) Wetting kinetics, kinematics and heat transfer characteristics of pongamia pinnata

- vegetable oil for industrial heat treatment. *Appl Therm Eng* 65(1–2):433–446
29. Grajcar A, Kilarski A, Kozłowska A (2018) Microstructure–property relationships in thermomechanically processed medium-Mn steels with high Al content. *Metals* 8(11):929
 30. Saha DC, Biro E, Gerlich AP, Zhou Y (2020) Martensite tempering kinetics: effects of dislocation density and heating rates. *Mater Charact* 168:110564

Publisher's note Springer Nature remains neutral with regard to jurisdictional claims in published maps and institutional affiliations.